

ELECTRICAL PROPERTIES OF SPHERICAL SYNCYTIA

R. S. EISENBERG, V. BARCILON, AND R. T. MATHIAS, *Department of Physiology,
College of Health Sciences, Rush University, Chicago, Illinois 60612 U.S.A.*

ABSTRACT Syncytial tissues consist of many cells whose intracellular spaces are electrically coupled one to another. Such tissues typically include narrow, tortuous extracellular space and often have specialized membranes at their outer surface. We derive differential equations to describe the potentials induced when a sinusoidal or steady current is applied to the intracellular space with a microelectrode. We derive solutions for spherical preparations with isotropic properties or with a particular anisotropy in effective extracellular and intracellular resistivities. Solutions are presented in an approximate form with a simple physical interpretation. The leading term in the intracellular potential describes an "isopotential" cell in which there is no spatial variation of intracellular potential. The leading term in the extracellular potential, and thus the potential across the inner membranes, varies with radial position, even at zero frequency. The next term of the potentials describes the direct effects of the point source of current and, for the parameters given here, acts as a series resistance producing a large local potential drop essentially independent of frequency. A lumped equivalent circuit describes the "low frequency" behavior of the syncytium, and a distributed circuit gives a reasonably accurate general description. Graphs of the spatial variation and frequency dependence of intracellular, extracellular, and transmembrane potential are given. The response to sinusoidal currents is used to calculate numerically the response to a step function of current.

INTRODUCTION

The electrical properties of cells and tissues are commonly measured by applying current to the cytoplasm with a microelectrode and recording the potential produced. The properties measured in this manner are properties of the entire preparation and are not simple measures of the properties of the components of the cell or tissue. In general, the observed electrical properties will depend on the paths of current flow, on the amount and structure of the membranes, and on the amount and structure of the intra- and extracellular spaces. The procedure for determining the electrical properties of the individual structures is fairly well known (Jack et al., 1975; Chandler and Schneider, 1976; Eisenberg et al., 1977): a circuit model of the preparation is constructed using the observed morphology of the preparation; the relation between the applied current and observed potential is derived for that model; the parameters of the model are determined by fitting the predictions of the theory to experimental data; finally, the model is tested against experimental data measured under a variety of conditions.

Although this procedure is well precededented in the case of preparations consisting of isolated cells, even with complex arrangements of membranes, it has not been widely used to analyze multicellular syncytia (see, however, Schoenberg et al., 1975; Eisenberg and Rae, 1976). Such multicellular preparations include two compartments: an intracellular com-

partment consisting of the cytoplasm of the cells and the junctions between cells and an extracellular compartment consisting of the extracellular space which infiltrates the tissue. Inasmuch as many important tissues are multicellular syncytia (lens of the eye: Rae, 1978; fat tissue: Sheridan, 1971; cultured cardiac cells: de Haan and Fozzard, 1975; natural cardiac tissues: Weidmann, 1966; liver: Haylett and Jenkinson, 1972; pancreas: Matthews and Sakamoto, 1975; salivary glands: Petersen, 1974; smooth muscle: Bennett, 1972; epithelia: Fromter, 1972), it seems worthwhile to attempt a systematic analysis of their electrical properties.

An analysis has been started by a number of workers (see Discussion). The present work was begun in collaboration with Dr. A. Peskoff, who has subsequently analyzed an expansion of the exact solution of a time-dependent version of this problem (Peskoff, 1978a).

This paper develops an analysis (Eisenberg et al., 1978) of the electrical properties of spherical tissues or cells with a pervading extracellular space. We begin with a general statement of the structure of such preparations and present a derivation of differential equations which in an approximate sense (analyzed in detail in a later paper) describe the spread of potential within the cells, within the extracellular space, and across the membranes of the preparation. A systematic procedure for solving these equations is developed, in which the general problem is broken into a series of physically well-defined problems, each usually easier to solve than the original problem. Solutions (usually in closed form) are given to each problem, and the solutions are presented graphically. The fit of these solutions to experimental data taken from the lens of the eye is presented in an accompanying paper (Mathias et al., 1979).

The analysis is presented in two parts. The first part presents the material of greatest relevance to experimental results, namely, a derivation of the differential equations, the physical meaning of the solutions, graphs of the properties of the solutions, a lumped equivalent circuit which represents the low frequency (long-time) properties of the solution, and finally a distributed equivalent circuit which has quite general validity. Second, there is a Methods section in which the solution of the equations (using perturbation theory) is outlined, and in which the solutions are presented in detail. Our attention is focused on the linear properties of tissues with spherical geometry, but the method of analysis is expected to apply to tissues and cells of other geometry. In the presence of nonlinearities, for example, voltage-dependent conductances in the membranes, the formal mathematical analysis breaks down, but there is every reason to expect that the qualitative properties of the analysis will not change because they are based on equivalent circuits with a physical meaning of their own, independent of their mathematical derivation.

GLOSSARY

Symbols used in the text are shown with units, definitions, and with reference to an equation using or defining them. **Boldface symbols** are used to indicate dimensionless quantities derived from dimensional quantities shown in *italics*, the normalization procedure being defined in and near Eqs. 25 and 26. Vector quantities are indicated by a superscript arrow.

a	Radius of the preparation. Eq. 15. (cm)
C_0	Defined in Eq. 46. (dimensionless)
C_1	See Eqs. 47, 51, and 52. (dimensionless)
C_m	Specific capacitance of the inner membranes. Eq. 8. (F/cm ²)

C_s	Specific capacitance of the surface membrane. Eq. 12. (F/cm ²)
$d\vec{S}$	Element of the surface identified below the integral sign. It is a vector of length dS pointing outwards from the surface. Eq. 1. (cm ²)
G_m	Specific conductance of the inner membranes. Eq. 8. (mho/cm ²)
G_s	Specific conductance of the surface membrane. Eq. 12. (mho/cm ²)
i_m	Modified spherical Bessel function defined in Eq. 54. (dimensionless)
$I_{m+1/2}$	Modified Bessel function of the first kind (Morse and Feshbach, 1953). Eq. 54. (dimensionless)
I_o	Amount of current applied to the preparation. Eq. 1. (A)
j	Equal to $\sqrt{-1}$. Eq. 13. (dimensionless)
\vec{J}_e	Current flux in the extracellular medium. Eq. 1. (A/cm ²)
$J_e^{(x)}$	The x component of the current flux \vec{J}_e . Eq. 3. (A/cm ²)
\vec{J}_i	Current flux in the intracellular medium. Eq. 1. (A/cm ²)
\vec{J}_m	Current flux across the inner membranes, outward current being positive. Eq. 2. (A/cm ²)
L^2	Angular component of the Laplacian defined in Eq. 62. (dimensionless)
m	Set of positive integers, starting with either $m = 0$ or $m = 1$, as indicated. Eq. 68. (dimensionless)
n	Set of positive integers, starting with either $n = 0$ or $n = 1$, as indicated. Eq. 37. (dimensionless)
$P_m(\cos \theta)$	Legendre polynomial (Morse and Feshbach, 1953). Eq. 53. (dimensionless)
r	Radial coordinate at which potential is measured. Eq. 13. (cm)
\vec{r}	Vector location at which potential is computed, the observation point. Eq. 7. (cm)
R	Radial coordinate of the source. Eq. 13. (cm)
\vec{R}	Vector location of the source. Eq. 7. (cm)
\vec{R}_0, \vec{R}_1	General position vectors. Eq. 55. (dimensionless)
R_e	(a) In the isotropic case the effective resistivity of the extracellular medium. Eq. 7. (b) In the anisotropic case the effective radial resistivity of the extracellular medium. Eq. 67. (ohm · cm)
R_i	(a) In the isotropic case the effective resistivity of the intracellular medium. Eq. 7. (b) In the anisotropic case the effective radial resistivity of the intracellular medium. Eq. 67. (ohm · cm)
R_j	Component of the effective intracellular resistivity produced by the junctions between cells. Eq. 7. (ohm · cm)
$R_s(r, R, \theta)$	Component of $U_i^{(1)}$ independent of frequency, or membrane properties. Eqs. 20 and 47. (ohm)
S_e	Surface of the extracellular medium on the face of the volume element ΔV . Eq. 1. (See Fig. 1.) (cm ²)
S_e/S_T	Ratio of the surface S_e to the surface of the face of the volume element ΔV . It is marked with a direction, e.g. $(S_e/S_T)_x$, in the anisotropic case. Eq. 3. (dimensionless)
S_i	Surface of the intracellular medium on the face of the volume element ΔV . Eq. 1. (See Fig. 1.) (cm ²)
S_m	Surface of all the membranes within the volume element ΔV . Eq. 2. (See Fig. 1.) (cm ²)
S_m/V_T	Surface of inner membrane in a unit volume of tissue. It is best to treat S_m/V_T as a single parameter. Eq. 9. (1/cm)
$U_e^{(0)}(r, j\omega)$	"Dominant" component of U_e . Eq. 21. (volt)
$U_e^{(1)}(r, R, \theta; j\omega)$	Component of U_e , the first order correction term. Eq. 21. (volt)
$U_e^{(n)}(\vec{r}, \vec{R})$	Set of extracellular "potentials" used to approximate U_e . Eq. 38. (dimensionless)
$U_e(r, R, \theta; j\omega)$	Average extracellular potential within a volume element. Eq. 5. (V)
$U_i(r, R, \theta; j\omega)$	Average intracellular potential within a volume element. Eq. 7. (V)
$\bar{U}_i(\vec{r}, \vec{R}; j\omega)$	Angular average of the potential $U_i^{(1)}$, defined in Eq. 63. (V)

$\tilde{U}_i(\mathbf{r}, \mathbf{R}, \theta; j\omega)$	Component of $U_i^{(1)}$ which varies with angular location, defined in Eq. 64. (V)
$U_i^{(0)}(j\omega)$	"Dominant" (isopotential) component of U_i . Eq. 13. (V)
$U_i^{(1)}(r, R, \theta; j\omega)$	Component of U_i , the first order correction. Eq. 13. (V)
$U_i^{(n)}(\vec{r}, \vec{R})$	Set of intracellular "potentials" used to approximate U_i . Eq. 37. (dimensionless)
$Y_e(j\omega)$	Specific admittance of the inner membranes when distributed along the extracellular resistance. Eq. 16. (mho/cm ²)
$Y_m(j\omega)$	Specific admittance of the inner membranes. Eq. 8. (mho/cm ²)
$Y_s(j\omega)$	Specific admittance of the surface membrane. Eq. 12. (mho/cm ²)

Greek Symbols

β_e	Ratio of the effective extracellular resistivity in the radial direction to that in the angular direction. Eq. 59. (dimensionless)
β_i	Ratio of the effective intracellular resistivity in the radial direction to that in the angular direction. Eq. 58. (dimensionless)
γ	Complex propagation constant. Eq. 17. (1/cm)
$\delta(\vec{r} - \vec{R})$	Vector Dirac delta function for a source at location \vec{R} . Eq. 27 writes $\delta(\vec{r} - \vec{R})$ in terms of its scalar components, in spherical coordinates with axial symmetry. (1/cm ³)
ΔV	Volume element of preparation, containing a representative sample of intra- and extracellular medium, illustrated in Fig. 1. Eq. 4. (cm ³)
Δx	Length in the x direction of the volume element ΔV . Eq. 3 and Fig. 1. (cm)
Δy	Length in the y direction of the volume element ΔV . Eq. 3 and Fig. 1. (cm)
Δz	Length in the z direction of the volume element ΔV . Eq. 3 and Fig. 1. (cm)
∇^2	Laplacian. The Laplacian is written explicitly in spherical coordinates with axial symmetry in Eqs. 58 and 62. (1/cm ² in dimensional equations; unitless in dimensionless equations)
ϵ	Equals $R_i/(R_i + R_e)$. Eq. 14. (dimensionless)
θ	Angular separation of source point and observation point. It is the "latitude" of one point, if the latitude of the other point is taken as zero. Eq. 13. (radians or deg)
κ	See Eq. 26. (dimensionless)
ν	See Eq. 69. (dimensionless)
σ_e	Conductivity of the solution filling the extracellular space within the preparation. Eq. 5. (mho/cm)
σ_i	Conductivity of the solution filling the intracellular space within the preparation. Eq. 7. (mho/cm)
τ_i, τ_e	Isotropic tortuosity factors for the intra- and extracellular media, respectively. Eq. 7. (dimensionless)
τ_{ex}	Tortuosity factor for the extracellular space, in the x direction. Eq. 5. (dimensionless)
ψ	Component of $U_i^{(1)}$. Eq. 19. (V)
ω	Angular frequency. Eq. 8. (rad/s)

RESULTS

Heuristic Derivation

Consider a tissue with a pervading extracellular space (Fig. 1), in contact with the surrounding bathing solution. Current is applied to the intracellular compartment through a microelectrode. The current must flow to the collecting (indifferent) electrode in the bath outside the tissue. It can flow through the intracellular space, across the membrane bounding the outside of the tissue, and to the bath electrode. Special properties conferred by the impedance of the couplings between cells will be subsumed into the effective properties of the cytoplasm. Or it can flow through the intracellular space, across the "inner"

membranes which separate the cytoplasm from the extracellular space, through the extracellular space, and out to the bath electrode. We consider the case where both flows of current are important and where the potentials induced within the cytoplasm and within the extracellular space are both significant, this case being the most general.

Consider a volume element ΔV much larger than a single cell of the tissue (Fig. 1). The current leaving the surface of that volume element can be written as the sum of the current leaving the surface of each medium (the intracellular medium is labeled with subscript i and the extracellular space with subscript e).

$$\int_{S_e} \vec{J}_e \cdot d\vec{S} + \int_{S_i} \vec{J}_i \cdot d\vec{S} = \begin{cases} I_0, & \text{if source is within } \Delta V \\ 0, & \text{if source is outside } \Delta V \end{cases} \quad (1)$$

where the currents are represented by the current flux vectors \vec{J}_e and \vec{J}_i . The surface integrals are taken over the surface defined under each integral sign. S_e is the surface of the extracellular medium on the face of the volume element; S_i is defined analogously (Fig. 1). the symbol $d\vec{S}$ is written to mean $\vec{n} dS$ where dS is an element of the surface over which the integral is performed and \vec{n} is a vector normal to the surface of unit length.

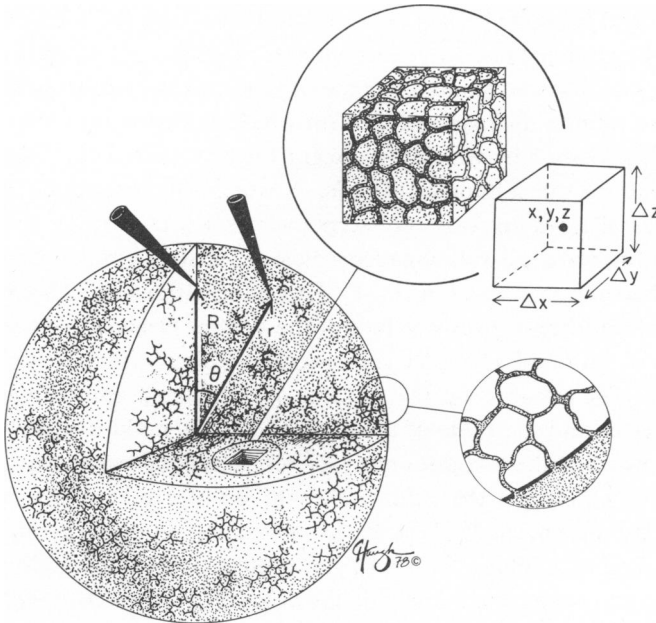


FIGURE 1 A spherical syncytium. The main figure emphasizes the spherical nature of the preparation and defines the locations of the source (namely, R) and of the point at which potential is measured, the observation point (r, θ). The gap junctions, which allow current to flow from the interior of any one cell to the interior of another, are not shown in the figure. One *inset* illustrates the special nature of the surface membrane and the relationship of the extracellular space to the exterior bathing solution. The other *inset* defines a volume element cut from the preparation. S_i is the area of the intracellular medium lying on the face of the cube, and S_e is the corresponding area of extracellular medium. The surface of inner membrane (with area S_m) is not shown in this *inset* because it lies within the volume element: the *inset* only illustrates faces of the element. The co-ordinates used to locate and define the volume element are Cartesian, for the sake of simplicity. The conversion to spherical coordinates is straightforward (Morse and Feshbach, 1953).

The sum of the currents leaving the extracellular space can also be derived from flux integrals because the inner membranes S_m and the surface S_e together form a closed boundary about the extracellular space in ΔV . (But the surface S_m of all the membranes within the volume element does not coincide with the surfaces on the faces of the volume element.) If the current source is not located within the extracellular space,

$$\int_{S_e} \vec{J}_e \cdot d\vec{S} - \int_{S_m} \vec{J}_m \cdot d\vec{S} = 0 \quad (2)$$

where \vec{J}_m describes the current flux across the internal membranes.

We proceed to derive equations describing a "smeared" (that is, average) representation of the potential within the intracellular and extracellular compartments of the tissue. We have explored four methods to derive such equations: (a) A rigorous but lengthy method by which the problem of potential spread in narrow invaginations is solved from first principles;¹ (b) a method by which the flux integrals in Eqs. 1 and 2 are converted into volume integrals using the divergence theorem and Ohm's law is then applied. This derivation suffered from ambiguities concerning the relationship of the specific and effective conductivities, particularly in the presence of anisotropies. See derivations of this type in Barr and Jakobsson (1976) and Peskoff (1978a); (c) a method by which the integrals are converted into the integral definition of the divergence operator (Schey, 1973), using the mean value theorem applied to an arbitrarily small volume of tissue. This derivation suffered from the consideration of an infinitesimal volume element which still contains both intra- and extracellular media; (d) a method by which the integrals are evaluated for a small piece of tissue, large enough to include a number of cells, in which the assumption is made that the flux (i.e., the potential) does not vary too steeply across any face of the piece of tissue (see Eq. 4). This latter form of the derivation seems most successful to us and is presented here.

Consider the first surface integral in Eq. 1. This integral consists of six surface integrals, each being the surface integral over one face of the volume element. We will evaluate the integrals on the $x + \frac{1}{2}\Delta x$ and $x - \frac{1}{2}\Delta x$ surfaces; the generalization to the other surfaces is straightforward. The integrals on the surfaces are evaluated approximately in terms of the area of the surface and the value of the integrand at the middle of the face. This procedure is correct provided the flux does not vary too steeply across the face of the volume element, there being no error if the volume element shrinks to zero size (see Schey, 1973, p. 38; and Morse and Feshbach, 1953, p. 35, for an evaluation of the error in general). Because we are restricted to a volume element large enough to include a representative sample of the intracellular and extracellular medium, the procedure is correct provided the flux does not vary too steeply in a distance of several cells.

For example, the x component of the flux integral for the surface of the extracellular space will then be

$$S_e [J_e^{(x)}(x + \Delta x/2, y, z) - J_e^{(x)}(x - \Delta x/2, y, z)] \\ = \Delta y \Delta z (S_e/S_T) [J_e^{(x)}(x + \Delta x/2, y, z) - J_e^{(x)}(x - \Delta x/2, y, z)], \quad (3)$$

¹Barcilon, V., R. S. Eisenberg, and R. T. Mathias. Microscopic and macroscopic description of the electrical properties of syncytial tissues. Manuscript in preparation.

the right-hand side of Eq. 3 is written in terms of S_T , the total surface of each x face of the volume element, which is $\Delta x \Delta y \Delta z$. Introducing the volume element $\Delta V = \Delta x \Delta y \Delta z$, we recognize a finite difference approximation to the partial derivative.

$$\Delta V \cdot (S_e/S_T)_x \frac{J_e^{(x)}(x + \Delta x/2, y, z) - J_e^{(x)}(x - \Delta x/2, y, z)}{\Delta x} \simeq \Delta V \cdot (S_e/S_T)_x \frac{\partial J_e^{(x)}}{\partial x}. \quad (4)$$

The surface ratio is marked with an x direction to allow the anisotropic case.

Ohm's law can now be introduced in the form

$$J_e^{(x)} = -\sigma_e \tau_{ex} \frac{\partial U_e}{\partial x}, \quad (5)$$

where σ_e is the conductivity of the extracellular space (mho/cm); U_e is the average potential in the extracellular space within the volume element; and the "tortuosity factor" τ_{ex} is introduced to take into account the branching and wiggling of the extracellular space. The tortuosity factor has been evaluated by Mathias et al. (1977) for planar branching networks of tubules in terms of experimentally measured morphometric parameters (see also Eisenberg et al., 1977, and Mathias et al., 1979).

Introduction of Ohm's law gives the expression for this component of the flux integral in terms of the potential.

$$\int_{z-\Delta z/2}^{z+\Delta z/2} dz \int_{y-\Delta y/2}^{y+\Delta y/2} J_e^{(x)} dy = -\Delta V \cdot (S_e/S_T)_x \tau_{ex} \sigma_e \frac{\partial^2 U_e}{\partial x^2}. \quad (6)$$

It is important to note that only one assumption has been used to introduce the smeared representation: the spatial variation of potential within a representative volume element is assumed to be sufficiently linear that spatial derivatives may be approximated by finite differences. In contrast to some of the other derivations mentioned previously, no discussion of an infinitesimal volume element is necessary and the morphometric parameters S_e/S_T and V_e/V_T are not confused.

The above treatment can be applied to each of the components of the surface integrals in Eq. 1. We write the result only for the isotropic case used in our later analysis. The anisotropic case is considered in Appendix II.

$$\frac{1}{R_e} \nabla^2 U_e + \frac{1}{R_i} \nabla^2 U_i = -I_0 \delta(\vec{r} - \vec{R}), \quad (7)$$

where the effective resistivities $R_i = R_j + 1/\{(S_i/S_T)\tau_i\sigma_i\}$ and $R_e = 1/\{(S_e/S_T)\tau_e\sigma_e\}$ are used for ease of notation. The delta function appears on the right-hand side as an approximation to $I_0/\Delta V$ for small ΔV . \vec{R} is the location of the source; \vec{r} is the point at which potential is measured.

The second integral in Eq. 2 is now to be evaluated. It can be written in terms of the potential across the membrane and the membrane admittance $Y_m = G_m + j\omega C_m$, where the admittance and membrane conductance G_m have units (mho/cm²), the membrane capacitance C_m has units (farad/cm²), $j = \sqrt{-1}$, and the angular frequency ω (rad/s) is 2π the frequency in hertz.

$$\int_{S_m} \vec{J}_m \cdot d\vec{S} = \int_{S_m} (U_i - U_e) Y_m dS \quad (8)$$

If we approximate the potentials by their value at the center of the volume element, this becomes

$$(S_m/V_T)[U_i(\vec{r}) - U_e(\vec{r})] Y_m \cdot \Delta V = \int_{S_m} \vec{J}_m \cdot d\vec{S}, \quad (9)$$

where S_m/V_T is the surface of membrane per unit volume of tissue. Then, Eq. 2 becomes

$$\nabla^2 U_e + R_e(S_m/V_T) Y_m (U_i - U_e) = 0, \quad (10)$$

which can be combined with Eq. 7 to give

$$\nabla^2 U_i - R_i(S_m/V_T) Y_m (U_i - U_e) = -I_0 R_i \delta(\vec{r} - \vec{R}). \quad (11)$$

The equations describing the spread of potential are made complete by the statement of the flow of current at the outer surface of the tissue. Current can leave the intracellular medium through the outer membrane of admittance $Y_s = G_s + j\omega C_s$, where the admittance and the membrane conductance have units reciprocal ohms per square centimeter and the membrane capacitance has units farads per square centimeter. There is no barrier to current flow at the outer edge of the extracellular space. Thus, we have the boundary conditions, discussed later in the paper,

$$\left. \begin{aligned} \frac{1}{R_i} \frac{\partial U_i}{\partial r} + Y_s U_i &= 0 \\ U_e &= 0 \end{aligned} \right\} \text{on } r = a. \quad (12)$$

Although the formulation used above seems to imply the existence of two potentials, U_i and U_e , at the same location, which would be rather puzzling, the derivation presented shows that such is not really the case. We will not be surprised, therefore, that a complete treatment of the spread of potential in the two media (see footnote 1) will give similar results for the partial differential equations but a distinctly different boundary condition.

Solutions

The solution to the problems posed in Eqs. 10, 11, and 12 has been determined using the techniques of perturbation theory, which have proven fruitful in related physiological problems (Barcilon et al., 1971; Peskoff and Eisenberg, 1975). The reader is referred to the Methods section for the details of our solution. Here we are concerned with those aspects of the solution which are of immediate use in describing a spherical syncytium.

The potential within the intracellular medium is written neglecting terms of order ϵ^2 (see Table I for value of ϵ).

$$U_i(r, R, \theta; j\omega) = U_i^{(0)}(j\omega) + \epsilon U_i^{(1)}(r, R, \theta; j\omega) \quad (13)$$

where

$$\epsilon = R_i/(R_i + R_e). \quad (14)$$

TABLE I
ELECTRICAL AND MORPHOLOGICAL PARAMETERS
OF LENS OF THE FROG EYE*

$G_s = 2.14 \cdot 10^{-4}$ mho/cm ²	$G_m = 4.38 \cdot 10^{-7}$ mho/cm ²
$C_s = 9.75$ μF/cm ²	$C_m = 0.79$ μF/cm ²
$R_i = 625$ ohm · cm	$R_e = 48.5$ kohm · cm
$S_m/V_T = 6 \cdot 10^3$ cm ⁻¹	$a = 0.16$ cm
Derived parameters*	
	$\epsilon = 0.013$
$\gamma(\text{DC}) = 1/880$ μm	$ \gamma(100 \text{ Hz}) = 1/26$ μm
$\kappa(\text{DC}) = 0.93$	$ \kappa(100 \text{ HZ}) = 0.79$

*Data from Mathias et al., 1979.

The first term $U_i^{(0)}(j\omega)$ describes the isopotential component of the intracellular potential, the component independent of spatial location, but dependent on membrane properties, and therefore frequency. This term describes the potential produced by current flow through a parallel combination of two admittances, $Y_s(j\omega)$ and $Y_e(j\omega)$, where $Y_s(j\omega)$ is the admittance of the surface membrane, a resistor and capacitor in parallel, and $Y_e(j\omega)$ is the admittance of the inner membranes when distributed along the extracellular resistance.

The first term of the intracellular potential is determined in the Methods section:

$$U_i^{(0)}(j\omega) = I_0/4\pi a^2(Y_s + Y_e) \quad (15)$$

where $Y_s(j\omega)$ has been defined near Eq. 12 and

$$Y_e(j\omega) = [\gamma/(R_i + R_e)](\coth \gamma a - 1/\gamma a) \quad (16)$$

with a = radius of spherical preparation

$$\gamma^2(j\omega) = (R_i + R_e)(S_m/V_T) Y_m. \quad (17)$$

Note that $\gamma(j\omega)$ is, at zero frequency, the reciprocal of a length constant as usually defined.

The physical nature of the distributed admittance $Y_e(j\omega)$ is of some general interest because it is analogous to the distributed admittance that arises in other physiological contexts, for example, the distributed admittance of the tubular system of skeletal muscle fibers. $Y_e(j\omega)$ is the ratio of the total current flowing out of the extracellular space to the potential across the surface membrane. This current flow equals the integral or sum of the currents flowing across the inner membranes.

If the extracellular and intracellular resistances were negligible, $\gamma a \rightarrow 0$ and the potential across the inner membranes would be spatially uniform and would equal the potential across the surface membrane. In general, however, γa is not near zero and the potential across the inner membranes is not spatially uniform, even though the intracellular potential is. Rather, there is substantial variation in the transmembrane potential because of the radial variation of the extracellular potential, arising from the long path length and high effective resistance of the extracellular medium.

The second term for the intracellular potential, $\epsilon U_i^{(1)}(r, R, \theta, j\omega)$, is numerically quite significant even at moderate frequencies and so cannot be neglected in our analysis. It is written

as the sum of two kinds of terms: (a) a frequency-independent term $R_s(r, R, \theta)$,² which acts as a series resistance independent of membrane properties but depending on position, position of the source, and internal resistance; and (b) frequency-dependent terms which depend on membrane properties (and therefore frequency), the radial location of source and observation point, but not on angular separation:

$$U_i^{(1)}(r, R, \theta, j\omega) = \psi(R, j\omega) + \psi(r, j\omega) - 2U_i^{(0)}(j\omega) + I_0 R_s(r, R, \theta), \quad (18)$$

where

$$\psi(r, j\omega) = U_i^{(0)}(j\omega) \frac{a}{r} \frac{\sinh \gamma r}{\sinh \gamma a} \quad (19)$$

$$R_s(r, R, \theta) = \frac{R_i + R_e}{4\pi a} \left\{ \left(\frac{r^2 + R^2}{a^2} - \frac{2rR}{a^2} \cos \theta \right)^{-1/2} + \left(1 + \frac{r^2 R^2}{a^4} - \frac{2rR}{a^2} \cos \theta \right)^{-1/2} - 2 + \log_e 2 - \log_e \left(1 - \frac{rR}{a^2} \cos \theta + \left[1 + \frac{r^2 R^2}{a^4} - \frac{2rR}{a^2} \cos \theta \right]^{1/2} \right) \right\} \quad (20)$$

The potential within the extracellular medium is written, neglecting terms of order ϵ^2 (see Table I),

$$U_e(r, R, \theta; j\omega) = U_e^{(0)}(r, j\omega) + \epsilon U_e^{(1)}(r, R, \theta; j\omega), \quad (21)$$

where, as is shown in the Methods section,

$$U_e^{(0)}(r, j\omega) = U_i^{(0)}(j\omega) \left(1 - \frac{a}{r} \frac{\sinh \gamma r}{\sinh \gamma a} \right). \quad (22)$$

Note that the first term of the extracellular potential is not spatially uniform, but varies only with radial location of the observation point. The radial variation of potential in the extracellular medium occurs because the current driven by the spatially uniform intracellular potential must flow through a large distributed extracellular resistance. The current flow in the extracellular space that produces $U_e^{(0)}$ is essentially the same current that flows through the admittance Y_e defined in the expression for $U_i^{(0)}$. The second term $U_e^{(1)}$ for the extracellular potential is sufficiently unwieldy to be relegated to the Methods section.

Graphic Results

It is of some practical interest to examine the spatial distribution of intracellular and extracellular potential computed under conditions of experimental relevance. The frequency dependence of the intracellular potential has been measured with a particular set of electrode locations (Mathias et al., 1979) for the lens of the eye, but not yet for other spherical syncytia

²The appearance of R_e in the expression for R_s is misleading because the contribution of R_s to the total observed potential is $I_0 R_s (R_i / (R_i + R_e))$. Thus, the contribution of the R_s term to the observed potential is independent of the extracellular resistivity.

like spherical preparations of cardiac muscle. Thus, the parameter values used must of necessity be those of the lens (Table I). On the other hand, there is little reason to believe that the qualitative electrical properties will differ when the parameters of other syncytia—with small extracellular space—are used, although undoubtedly the natural frequency and other quantitative behavior will differ.

First, consider the spatial variation of intracellular and extracellular potential when sinusoidal or steady current is applied in the center of the preparation. Fig. 2 shows this variation, intracellular potential on the left and extracellular potential on the right. Each panel is computed at the frequency indicated; the dashed lines indicate the first component of potential, namely, $U_i^{(0)}$ or $U_e^{(0)}$; the solid lines indicate the "total" potential $U_i = U_i^{(0)} + \epsilon U_i^{(1)}$ or $U_e = U_e^{(0)} + \epsilon U_e^{(1)}$, if 1 μ A of current were applied. In the sinusoidal case the potential is described by a complex number. The real part of the potential is plotted because the real part describes the amplitude of a sinusoidal voltage at some definite time, whereas the magnitude of the complex potential does not describe such a physical voltage.

The curves in Fig. 2 also illustrate the spatial variation of the real part of the "input" impedance or "input" resistance (at zero frequency) at different frequencies for the current electrode locations shown. In the uppermost panels, computed for zero frequency, the effect of the point source is clearly seen in the intracellular potential, producing a singularity at $r = 0$ and dominating the potential for a substantial region around the center of the preparation. The isopotential component of intracellular potential is dominant away from the point source, as expected. The extracellular potential under these conditions shows hardly a trace of the point source. It is essentially the response of the extracellular medium to the isopotential component of the intracellular potential. Such is the case because the values of the resistance of the internal membranes in the lens are high enough to insulate the extracellular medium from the effects of the singularity in the intracellular potential. The inner membranes, however, are not perfect insulators; indeed, it is the current that crosses those inner membranes which produces the extracellular potential shown in the graph. Note that the amplitude of the extracellular potential is comparable to that of the intracellular potential; thus, the voltage across the inner membranes—the difference of the intracellular and extracellular potentials—varies quite significantly across the preparation, even at zero frequency. The lower panels in the figure show similar plots of the spatial variation of potential at higher frequencies. Note that as frequency increases, the spatially uniform component of potential decreases. This is because the admittance of the membranes becomes primarily capacitive and is therefore increasing linearly with frequency. A component of intracellular potential directly produced by the point source does not change with frequency, as expected from the frequency independence of the series resistance component of $U_i^{(1)}$. The fact that $U_i^{(1)}$ itself is fairly independent of the frequency implies that, for the parameters of the lens, the series resistance term dominates the other components of $U_i^{(1)}$. The effect of frequency on the extracellular potential is more interesting. First, note that the extracellular potential becomes larger compared to the intracellular potential. This is to be expected because one component of the intracellular admittance is produced by the surface capacitance. The comparable component of the extracellular admittance arises from a distributed admittance in which almost all the (inner) membranes are in series with a portion of the extracellular resistance. Furthermore, the effect of the point source on the extracellular

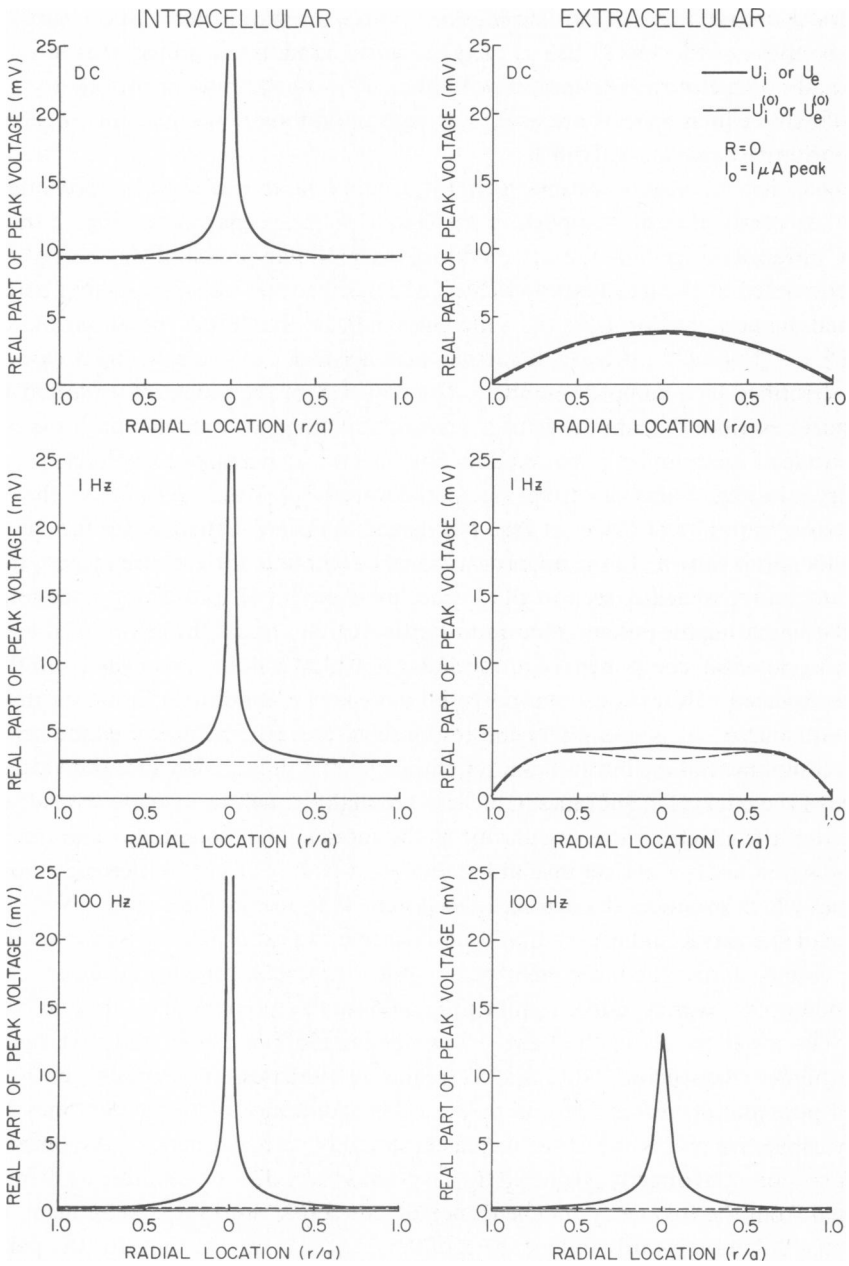


FIGURE 2 The spatial variation of potential. The graphs illustrate the real part of the peak voltage induced by a sinusoidal current of $1 \mu A$ (peak) applied with a point source to the center of the preparation. The ordinate can also be read as the real part of the impedance (or, at DC, input resistance) in units of kilo-ohms. The solid line describes the "total" potentials U_i or U_e , the dashed lines indicate the $U_i^{(0)}$ or $U_e^{(0)}$. The left-hand panels illustrate the spatial variation of intracellular potential, at the frequencies indicated in each panel. The right panels illustrate the radial variation of extracellular potential. The figures were computed using Eqs. 13–22 and 51 with parameter values specified in Table I and on the figure itself. The dependence on frequency is subject to uncertainties described in the Discussion.

resistance becomes quite marked as frequency increases. Indeed, at 100 Hz the extracellular potential is quite close to the intracellular potential in most of the preparation. At 100 Hz the admittance of the inner membranes has increased enough so that they no longer shield the extracellular medium from the effects of the point source in the intracellular medium.

Fig. 3 illustrates that moving the point source away from the center of the preparation has no marked effect on the qualitative properties of the intracellular potential. The two panels show that the spatial dependence and frequency dependence of the several components are similar to those already seen.

The dependence of the intracellular potential on frequency is also of considerable interest because it is that dependence which is determined in experimental measurements of impedance. Fig. 4 shows the dependence of the magnitude and phase of the impedance on frequency for two locations of the electrodes; note that in these cases both electrodes are just under the surface of the preparation, as is often the case experimentally (Eisenberg and Rae, 1976). Calculations with one electrode in the center give qualitatively similar results, but with smaller values of the series resistance, as would be expected from Fig. 2. It is interesting to note that the dependence of magnitude of the impedance on frequency is qualitatively similar to that of a simple parallel circuit of a resistor and capacitor. The dependence of the phase angle is quite different, however, illustrating the greater sensitivity of the phase function to the properties of an electrical model.

The theory developed here allows the estimation of the response of the preparation to a step function of current. The impedance U_i/I_0 is multiplied by the Fourier transform of an "on-then-off" step of current, and the inverse Fourier transform is approximated by a numerical discrete inverse Fourier transform (Brigham, 1974). The intracellular voltage after the onset of current is shown in Fig. 5. These results illustrate the step response produced by the first two terms of the perturbation expansion. They cannot be rigorously

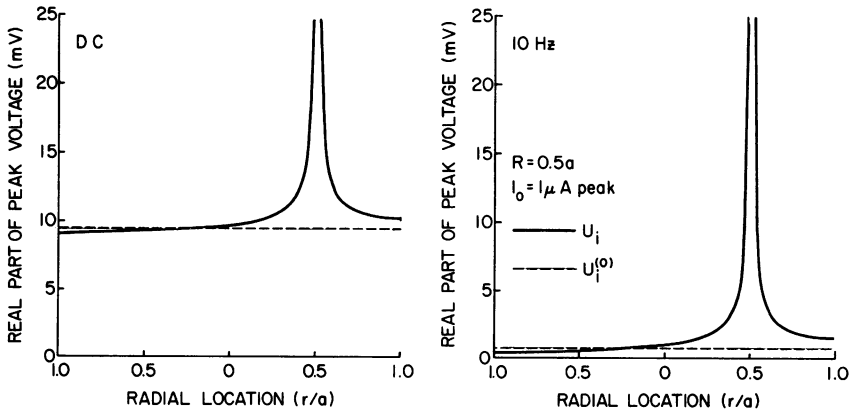


FIGURE 3 The spatial variation of intracellular potential. The graphs illustrate the real part of the peak voltage induced by a sinusoidal current of $1 \mu\text{A}$ (peak) applied with a point source to a location halfway between the center and edge of the preparation. The ordinate can also be read as the real part of the impedance (or, at DC, the input resistance) in units of kilo-ohms. The figures were computed using Eqs. 13–20 with parameters specified in Table I and on the figure itself. The solid lines describe the "total" potential U_i and the dashed line the component of potential $U_i^{(0)}$. The dependence on frequency is subject to uncertainties described in the Discussion.

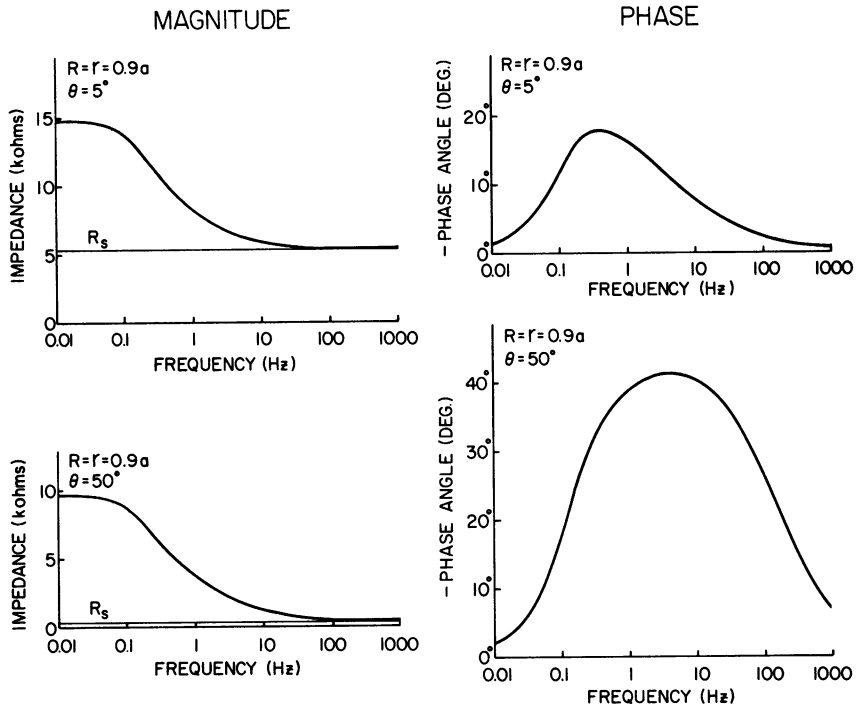


FIGURE 4 The frequency dependence of the approximate solution. The panels illustrate the frequency dependence of the total intracellular impedance U_i/I_0 (solid line) and the series resistance R_s (dashed line). The location of the point source and the point at which potential is measured is shown on each panel. The left-hand panels illustrate the magnitude of the impedance and the right-hand panels illustrate the phase angle of the impedance. The dependence on frequency is subject to uncertainties described in the Discussion.

equated with the step response of the preparation, although in an analogous case that equality has been shown (Peskoff and Eisenberg, 1975).

Summary of Results and Approximate Representation as Circuits

The electrical properties of a spherical syncytia that are of most interest physiologically can be summarized by Eq. 23:

$$U_i/I_0 = [1/4\pi a^2(Y_s + Y_e)] + \epsilon R_s(r, R, \theta) + [\epsilon/4\pi a^2(Y_s + Y_e)]\{(a/\sinh \gamma a)(\sinh \gamma r/r + \sinh \gamma R/R) - 2\}, \quad (23)$$

where Y_s and Y_e are defined in Fig. 6 and Eq. 16, γ is defined in Eq. 17, ϵ is defined in Eq. 14, and $R_s(r, R, \theta)$ is defined in Eq. 20. In the case that the length constant is much greater than the radius of the preparation ($\gamma a \rightarrow 0$), a simple lumped circuit, usually called (somewhat loosely) the "low frequency approximation," can be written (Fig. 6). In the case that the rightmost term of Eq. 23 is negligible, a more accurate approximate circuit can be written as well (Fig. 6).

The accuracy of the equivalent circuit representations depends, of course, on the value of ϵ . In the case of the lens of the frog eye, the last term in Eq. 23 is negligible, so the

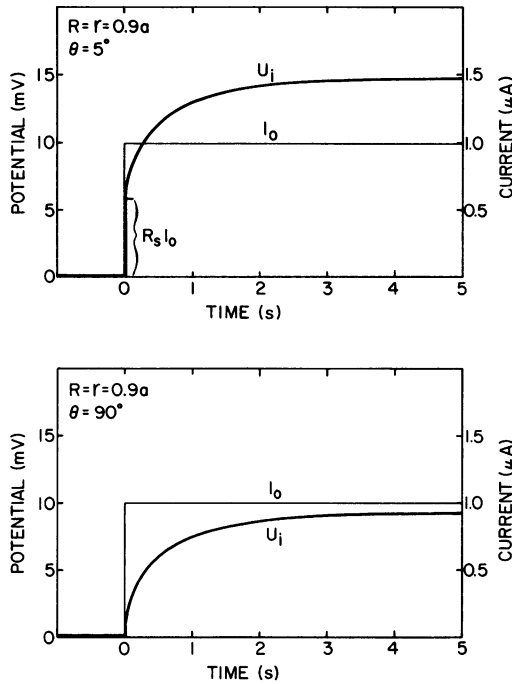


FIGURE 5 The step function response. The response predicted from Eq. 13 to a step function of current is shown for two different locations. Note the “jump” in potential at close electrode separations, the exponential time-course of the slow rise in potential and the equality of the slow component of potential at different positions. These properties, predicted by the model and illustrated here, have been found experimentally by Eisenberg and Rae (1976), in the lens of the frog eye, within the uncertainties described in the Discussion.

distributed approximation is quite an accurate representation; in other preparations, for example, spherical preparations of cardiac muscle, the parameters have not been measured to determine the accuracy of the approximations. In any case, however, the circuits are likely to yield physical insight which may be difficult to gain directly from the mathematical expressions.

Both of these circuits include the series resistance ϵR_s , which reflects the effects of the flow of current near the point source. If both electrodes are just under the surface of the preparation ($r = R = a$), then an expression for ϵR_s is

$$\epsilon R_s = \frac{R_i}{4\pi a} \left[\frac{1}{\sin \theta/2} - 2 - \log_e \{(\sin \theta/2)(1 + \sin \theta/2)\} \right]; \text{ for } r = R = a \quad (24)$$

which for sufficiently small angular separation becomes

$$\epsilon R_s \rightarrow \frac{R_i}{2\pi a\theta} \text{ for } \theta \rightarrow 0; \quad r = R = a.$$

If one electrode is just under the surface, i.e. $(a - r)/a$ is small, and the other electrode is near the center of the preparation (i.e. R/a is small), then we have another approximate

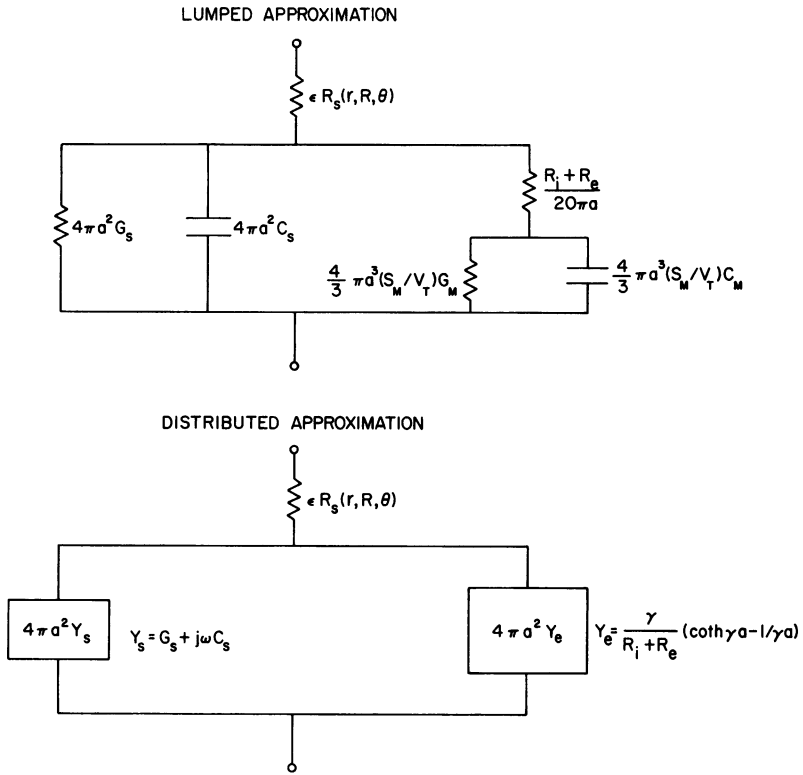


FIGURE 6 Circuit approximations to the electrical model. The left-hand circuit is a circuit approximation valid when γa is small. The series resistance is defined precisely in Eq. 20 and approximated for special cases in and near Eq. 24. The distributed circuit approximation is more accurate (for parameters defined in Table I) over the physiological range of frequencies, subject to the uncertainties described in the Discussion.

expression for R_s ,

$$\epsilon R_s \simeq \frac{R_i}{4\pi a} \left(\frac{a-r}{a} + \frac{3R}{a} \cos \theta \right) \text{ for } \begin{cases} \frac{a-r}{a} \ll 1 \\ \frac{R}{a} \ll 1 \end{cases}$$

where terms of order $(R/a)^2$, $(a-r)^2/a^2$, and $R(a-r)/a^2$ have been neglected.

METHODS

Expansions

The solution to the problems posed by Eqs. 10, 11, and 12 is determined by first writing the problems in normalized form to isolate the dimensionless parameters of the system and to determine their sizes. We use the dimensionless variables, shown in bold face type,

$$U_i = \frac{U_i}{\gamma I_0 (R_i + R_e)}; \quad U_e = \frac{U_e}{\gamma I_0 (R_i + R_e)} \quad (25)$$

$$\epsilon = \frac{R_i}{R_i + R_e}; \quad \kappa = \frac{\gamma(Y_s/Y_m)}{S_m/V_T} \quad (26)$$

with the length scale set by the natural "length" $1/\gamma$ defined previously (Eq. 17).

The normalized equations are written in terms of the dimensionless spatial variables $\mathbf{r} = \gamma\mathbf{r}$ and $\mathbf{R} = \gamma\mathbf{R}$. The Laplacian ∇^2 in dimensionless coordinates equals the Laplacian in dimensional coordinates divided by γ^2 ; $\delta(\vec{\mathbf{r}} - \vec{\mathbf{R}}) = \gamma^2\delta(\vec{\mathbf{r}} - \vec{\mathbf{R}})$. The differential equations then become

$$\nabla^2 U_i - \epsilon(U_i - U_e) = -\epsilon\delta(\vec{\mathbf{r}} - \vec{\mathbf{R}}) = -\epsilon\delta(\mathbf{r} - \mathbf{R})\delta(\theta)/(2\pi r^2 \sin \theta), \quad (27)$$

$$\nabla^2 U_e + (1 - \epsilon)(U_i - U_e) = 0, \quad (28)$$

$$\left. \begin{aligned} \frac{\partial U_i}{\partial r} + \kappa U_i &= 0 \\ U_e(\gamma a) &= 0 \end{aligned} \right\} \text{on } \mathbf{r} = \gamma a. \quad (29)$$

The use of a complex number to represent a dimensionless length may seem somewhat nonphysical. The definition of such a complex length scale is natural in the theory of transmission lines, where the use of the propagation constant leads to much physical insight. In our case, because the equations are linear, both the length scales and the cell size (and all other distances) are multiplied by the same complex number. Thus, the statement $\mathbf{r} = \gamma a$ means that the dimensional location $r = a$.

The definitions of the length scale $1/\gamma$ and the small parameter ϵ both differ from those used in problems describing single spherical cells. The length scale chosen here depends on the electrical properties of the membranes and preparation, not on its size. The small parameter isolated here depends on the effective resistivities of the intracellular and extracellular media (that is, on the resistivities, the morphometric parameters, and the connectivity of these media and on the resistance of the junctions between cells), but not on the properties of the membranes. Thus, our ϵ does not vary as the admittance of the membrane changes, neither because of nonlinearities in the membrane capacitance or conductance nor because of frequency dependence introduced by the membrane capacitance. This choice of parameters was motivated by experience with related electrical problems describing networks like one-dimensional cables. The choice was confirmed by the solution of a simplified form of our problem with the current source in the center of the preparation, which showed that the first three terms of the perturbation expansion are the entire exact solution. Perhaps the use of such parameters, particularly of an electrical instead of a geometrical length scale, would simplify other problems (Peskoff et al. 1976). Typical values of the parameters ϵ , κ , and $1/\gamma$ are given in Table I, based on the measured properties of the lens of the eye (Mathias et al., 1979). Values for another spherical syncytium—of cultured cardiac cells—are unfortunately not available.

The next step in the analysis is to construct an expansion in the small parameter. The expansion will proceed in integral powers of ϵ , because the coupling between terms in the Eqs. 27–30 insures that terms in the expansion multiplied by fractional powers of ϵ would be identically zero. Furthermore, the expansions for U_i and U_e must start with the same order or no consistent (i.e., well posed) set of problems can be derived. The definition of the "input" or normalizing resistance $(R_i + R_e)\gamma$ is somewhat more arbitrary; other definitions lead to expansions of the normalized potentials which appear at first blush to be of different form, but which become identical when written in dimensional form.

The resulting expansions are

$$U_i(\vec{\mathbf{r}}, \vec{\mathbf{R}}; \epsilon) = U_i^{(0)}(\vec{\mathbf{r}}, \vec{\mathbf{R}}) + \epsilon U_i^{(1)}(\vec{\mathbf{r}}, \vec{\mathbf{R}}) + \dots \quad (31)$$

$$U_e(\vec{\mathbf{r}}, \vec{\mathbf{R}}; \epsilon) = U_e^{(0)}(\vec{\mathbf{r}}, \vec{\mathbf{R}}) + \epsilon U_e^{(1)}(\vec{\mathbf{r}}, \vec{\mathbf{R}}) + \dots \quad (32)$$

Sequences of problems are determined by substituting these expansions into the differential equa-

tions and boundary conditions and collecting terms of the same power in ϵ . The collection procedure is an easier way of performing a systematic limit process in which the case of $\epsilon \rightarrow 0$ is considered to determine the first problems $U_i^{(0)}$ and $U_e^{(0)}$. These potentials are then subtracted from the equations which describe the total potential and the case of $\epsilon \rightarrow 0$ is again considered, giving the problems $U_i^{(1)}$ and $U_e^{(1)}$ for the first order correction. Repetition of this process generates all the higher order terms.

The first of the sequence of problems is, for the intracellular medium,

$$\begin{aligned}\nabla^2 U_i^{(0)} &= 0 \\ \frac{\partial U_i^{(0)}}{\partial \mathbf{r}} &= 0 \text{ on } \mathbf{r} = \gamma a\end{aligned}\quad (33)$$

and for the extracellular medium,

$$\begin{aligned}\nabla^2 U_e^{(0)} - U_e^{(0)} &= U_i^{(0)} \\ U_e^{(0)} &= 0 \text{ on } \mathbf{r} = \gamma a.\end{aligned}\quad (34)$$

The next problems are then, for the intracellular medium,

$$\begin{aligned}\nabla^2 U_i^{(1)} &= -\delta(\mathbf{r} - \mathbf{R}) + U_i^{(0)} - U_e^{(0)} \\ \frac{\partial U_i^{(1)}}{\partial \mathbf{r}} &= -\kappa U_i^{(0)}; \text{ on } \mathbf{r} = \gamma a,\end{aligned}\quad (35)$$

and for the extracellular medium,

$$\begin{aligned}\nabla^2 U_e^{(1)} - U_e^{(1)} &= U_i^{(0)} - U_e^{(0)} - U_i^{(1)} \\ U_e^{(1)} &= 0; \text{ on } \mathbf{r} = \gamma a.\end{aligned}\quad (36)$$

The assignment of the delta function to the second order approximation (the order ϵ problem) might appear strange because an infinitely large "function" then appears in a problem specifying a correction term. However, the appearance of the delta function in the $U_i^{(1)}$ problem is neither arbitrary nor fortuitous; assignment of the delta function to another order problem leads either to inconsistencies (if the assignment is to the order zero problem) or to trivial restatements of the present expansions (if the assignment is to order two or higher problems).

Finally, the problems for the higher order potentials are, for the intracellular case,

$$\left. \begin{aligned}\nabla^2 U_i^{(n)} &= U_i^{(n-1)} - U_e^{(n-1)} \\ \frac{\partial U_i^{(n)}}{\partial \mathbf{r}} &= -\kappa U_i^{(n-1)}; \text{ on } \mathbf{r} = \gamma a\end{aligned}\right\} n \geq 2 \quad (37)$$

and for the extracellular case,

$$\begin{aligned}\nabla^2 U_e^{(n)} - U_e^{(n)} &= U_i^{(n-1)} - U_e^{(n-1)} - U_i^{(n)} \\ U_e^{(n)} &= 0; \text{ on } \mathbf{r} = \gamma a\end{aligned} \quad n \geq 1. \quad (38)$$

In the derivation of the problems κ is assumed to be order 1, as is the physiological case, and as is required if the perturbation expansion is to be useful.

We would like to proceed to solve these problems one at a time, taking the problem for the intracellular medium before that of the extracellular medium. However, it is clear that the problems stated are not well posed (that is, do not have a unique solution), because a constant could be added

to each of the potentials in Eqs. 33, 35, and 37 and still be a solution. $U_i^{(0)}$ will in fact be specified by the requirement that the problem for $U_i^{(1)}$ be consistent, namely, that the total current leaving the preparation (the surface integral of the radial derivative of the potential) equal the current leaving the source. Integrating the equation for $U_i^{(1)}$ gives, with dV as the volume element,

$$\iiint_{\text{tissue}} \nabla^2 U_i^{(1)} dV = -1 + \iiint_{\text{tissue}} (U_i^{(0)} - U_\varepsilon^{(0)}) dV. \quad (39)$$

Application of the divergence theorem (Schey, 1973) and the boundary condition gives the integral constraint which specifies the problem for $U_i^{(0)}$

$$\kappa \iint_{\text{surface}} U_i^{(0)} dS = 1 - \iiint_{\text{tissue}} (U_i^{(0)} - U_\varepsilon^{(0)}) dV. \quad (40)$$

Similar integration and treatment of the higher order problems give the integral constraint for the problem for $U_i^{(n)}$, $n \geq 1$

$$\kappa \iint_{\text{surface}} U_i^{(n)} dS = - \iiint_{\text{tissue}} (U_i^{(n)} - U_\varepsilon^{(n)}) dV; \quad n \geq 1. \quad (41)$$

These integral constraints, together with the statement of the problems, Eqs. 33–38, now specify the sequence of approximations $U_i^{(0)}$, $U_i^{(1)}$, ... and $U_\varepsilon^{(0)}$, $U_\varepsilon^{(1)}$, ...

Another version of the integral constraints can be derived by integration of the differential equations which specify $U_\varepsilon^{(n)}$ and substitution from Eq. 40 or 41:

$$\kappa \iint_{\text{surface}} U_i^{(0)} dS - \iint_{\text{surface}} \frac{\partial U_\varepsilon^{(0)}}{\partial r} dS = 1 \quad (42)$$

$$\kappa \iint_{\text{surface}} (U_i^{(0)} - U_i^{(1)}) dS + \iint_{\text{surface}} \frac{\partial U_\varepsilon^{(1)}}{\partial r} dS = 1 \quad (43)$$

$$\kappa \iint_{\text{surface}} (U_i^{(n-1)} - U_i^{(n)}) dS + \iint_{\text{surface}} \frac{\partial U_\varepsilon^{(n)}}{\partial r} dS = 0; \quad n \geq 2. \quad (44)$$

Although these forms of the integral constraints are not needed in a minimal specification of the problems for the intracellular and extracellular potentials, they (together with the other forms of the constraints) are helpful in understanding the relationship of the current flows across the surface membrane, the inner membranes, and out of the extracellular space. Examination of Eqs. 40 and 41 shows that current flow across the surface membrane in a problem of order n appears in its entirety as current flow across the inner membranes in the problem of the same order n . Examination of Eqs. 42–44, however, shows that current flow out of the extracellular space in a problem of order n is produced by surface membrane current (or equivalently, inner membrane current) of two different orders. Thus, there is a coupling between current flows in the different orders of approximation; all the current flows do not balance in a set of problems of a single order. Finally, examination of the integral constraints shows that the source term appears explicitly only in the constraints derived from the $n = 0, 1$ problems. This property of the constraints probably is related to the termination of the exact solution in just three terms for the case where $\mathbf{R} = 0$.

Solutions

Consider the problem defining $U_i^{(0)}$. The absence of a driving force (an inhomogeneous term on the right-hand side) for the differential equation and boundary condition implies

that $U_i^{(0)}$ is spatially uniform, described by the constant $U_i^{(0)} = C_0$. Note that the "constant" C_0 can, and does in fact, depend on membrane properties and therefore frequency.

The problem for $U_i^{(0)}$ is easily solved because the driving force (the right-hand side) is spherically symmetric, making $U_i^{(0)}$ a function only of r . The resulting ordinary differential equation has the solution

$$U_i^{(0)} = C_0 \left[1 - \frac{\gamma a}{r} \frac{\sinh r}{\sinh \gamma a} \right]. \quad (45)$$

Substitution of the expression for $U_i^{(0)}$ into the integral constraint (Eq. 40) allows determination of $U_i^{(0)}$:

$$U_i^{(0)} \equiv C_0 = \{4\pi(\gamma a)^2(\kappa + \coth \gamma a - 1/\gamma a)\}^{-1}. \quad (46)$$

We next turn to the problem for $U_i^{(1)}$ with the understanding that determination of the solution will require consideration of the integral constraint (Eq. 41) and thus the problem for $U_i^{(1)}$. It saves considerable labor to separate the potential into parts. Note that R_s , unlike the other components of U_i in Eq. 18, is defined as a resistance (in units of ohms). Its dimensionless counterpart is defined as $\mathbf{R}_s = R_s/\gamma(R_i + R_e)$.

$$U_i^{(1)} = \mathbf{R}_s(\mathbf{r}, \mathbf{R}, \theta) + \psi(\mathbf{r}) + \psi(\mathbf{R}) + C_1, \quad (47)$$

where $\psi(\mathbf{R})$ and C_1 are constants in the sense that they are independent of \mathbf{r} and θ . The appearance of $\psi(\mathbf{R})$ is guaranteed by the reciprocity theorem proven in Appendix I. The constant C_1 is chosen later to satisfy the integral constraint. The specification of these problems is somewhat arbitrary. The integral constraint on \mathbf{R}_s was chosen to make the problem identical with that solved in Barcilon et al. (1971). The boundary value $\psi(\gamma a) = C_0$ was chosen for simplicity; we knew that any value was acceptable because it would simply be accommodated by a different value of C_1 . In retrospect, it would seem better to have defined a boundary value so that C_1 would have been zero. In that case $\psi^{(n)}$, the n^{th} -order generalization of ψ , would have been just $-U_i^{(n-1)}$, and the structure of the solutions would have been clearer.

$$\left. \begin{aligned} \nabla^2 \mathbf{R}_s &= -\delta(\vec{\mathbf{r}} - \vec{\mathbf{R}}) \\ \frac{\partial \mathbf{R}_s}{\partial r} &= \frac{-1}{4\pi(\gamma a)^2} \text{ on } r = \gamma a \\ \iint_{\text{surface}} \mathbf{R}_s dS &= 0 \end{aligned} \right\} \quad (48)$$

and

$$\left. \begin{aligned} \nabla^2 \psi &= C_0 - U_i^{(0)} \\ \frac{\partial \psi}{\partial r} &= -\kappa C_0 + \frac{1}{4\pi(\gamma a)^2} \\ \psi &= C_0 \end{aligned} \right\} \text{ on } r = \gamma a \quad (49)$$

The dimensional form of $\mathbf{R}_s(r, R)$ is given in Eq. 20. The form has been derived by Barcilon et al. (1971, Eq. 26)³ and is discussed in Sobolev (1964, p. 297) and Kellogg (1929, p. 247).

The functional form of ψ is easy to determine because C_1 is independent of location and $U_\varepsilon^{(0)}$ depends only on r , not θ . The Laplacian in Eq. 49 then becomes an ordinary differential operator and the solution of Eq. 49 is easily found to be (see Eq. 19)

$$\psi(\mathbf{r}) = C_0 - U_\varepsilon^{(0)} = C_0 \left(\frac{\gamma a}{r} \right) \left(\frac{\sinh r}{\sinh \gamma a} \right). \quad (50)$$

The remaining constant C_1 must now be chosen from the integral constraint (Eq. 43), which involves the functional form for $U_\varepsilon^{(1)}$. That form is considerably simplified, however, as C_1 is independent of \mathbf{R} . Then, we need only consider the case of $\mathbf{R} = 0$.

We now turn to the problem for $U_\varepsilon^{(1)}$ with $\mathbf{R} = 0$. The Laplacian again becomes an ordinary differential operator, and the solution can be easily found:

$$U_\varepsilon^{(1)}(\mathbf{r}, 0) = \left(C_1 + C_0 \frac{\gamma a}{\sinh \gamma a} - \frac{1}{4\pi \gamma a} \right) \left(1 - \frac{\sinh r}{r} \frac{\gamma a}{\sinh \gamma a} \right) + \frac{1}{4\pi r} \left(1 - e^{-r} - \frac{\sinh r}{\sinh \gamma a} [1 - e^{-\gamma a}] \right). \quad (51)$$

Application of the integral constraint (Eq. 43) shows, after a certain amount of algebraic manipulation involving repeated use of Eq. 46, that

$$C_1 = -2C_0. \quad (52)$$

This component of the extracellular potential has also been determined in general and shown to satisfy the integral constraint for all values of \mathbf{R} .

$$U_\varepsilon^{(1)}(\mathbf{r}, \mathbf{R}, \theta) = \mathbf{R}_s(\mathbf{r}, \mathbf{R}, \theta) + [C_1 + \psi(\mathbf{R})][1 - \psi(\mathbf{r})/C_0] - \frac{1}{4\pi} \sum_{m=1}^{\infty} \frac{2m+1}{m} \frac{\mathbf{R}^m}{(\gamma a)^{m+1}} \frac{i_m(\mathbf{r})}{i_m(\gamma a)} P_m(\cos \theta) + \frac{1}{4\pi} \sum_{m=0}^{\infty} (-1)^m (2m+1) i_m(\mathbf{R}) i_m(\mathbf{r}) \left[\frac{i_{-m-1}(\gamma a)}{i_m(\gamma a)} - 1 \right] P_m(\cos \theta) - \frac{\exp(-|\vec{\mathbf{r}} - \vec{\mathbf{R}}|)}{4\pi |\vec{\mathbf{r}} - \vec{\mathbf{R}}|}, \quad (53)$$

where $P_m(\cos \theta)$ is a Legendre polynomial and the modified spherical Bessel functions i_m are defined in terms of the more conventional modified Bessel functions $I_{m+1/2}$:

$$i_m(\mathbf{r}) \equiv \sqrt{\frac{\pi}{2\mathbf{r}}} I_{m+1/2}(\mathbf{r}) \quad (54)$$

and where $|\vec{\mathbf{r}} - \vec{\mathbf{R}}| = (\mathbf{r}^2 + \mathbf{R}^2 - 2\mathbf{r}\mathbf{R} \cos \theta)^{1/2}$.

³The reader should be aware that the dimensionless spatial variables of Barcilon et al. are not identical to those used here.

DISCUSSION

Historical Comments

The spread of potential in two interdigitating media has been considered in two different biological contexts: the context of skeletal muscle, with its T-system which invaginates the cylindrical fiber, and the context of syncytia, with its pervading extracellular space. The analysis of syncytia, particularly of spherical shape, has either assumed a discrete network (see references in Purves, 1976) or assumed that current can flow into the extracellular medium in every small region of the syncytium. Shaw (1964) derived a partial differential equation of the Klein-Gordon form (i.e., the form of our Eq. 11 if $U_e = 0$) from this physical consideration. Adrian (personal communication, ca. 1969), Jack et al. (1975, Chap. 5); and Purves (1976) solved this equation with various boundary conditions (not equivalent to ours) in various special cases. This work did not deal explicitly with the separate intracellular and extracellular potentials, but rather tried to analyze the transmembrane potential $U_i - U_e$, assuming it equaled the intracellular potential U_i . Such an analysis is inappropriate when $U_e = 0$.

Recently, a more explicit approach, involving the potential in both the extracellular and intracellular media has been used (Barr and Jakobsson, 1976; Peskoff, 1978*a*). The former paper uses rather different boundary conditions; the latter paper presents an exact solution of a time domain version of the problem defined here. The exact solution has obvious advantages; the advantages of a perturbation approach have been discussed at length (Peskoff and Eisenberg, 1973). Briefly, the perturbation approach permits construction of a systematic computable set of physical approximations, which permits construction of an equivalent circuit representation, and which permits easy generalization to related problems of more complex geometry or electrical behavior. The disadvantage of a perturbation approach lies in the possibility of nonuniformities in the convergence of the resulting expansion. Such nonuniformities occur, in the same manner, in expansions of the exact solution in a small parameter (as used by Peskoff, 1978*a, b*).

The analysis of skeletal muscle with T-system has been done in a more physical, less rigorous way. Falk and Fatt (1964) proposed that the main effect of the T-system was to provide an alternative path by which current could leave the sarcoplasm; the T-system did not interfere with the longitudinal current flow, rather it simply added an admittance in parallel with that of the surface membrane. This admittance was calculated with a radial and "inside-out" version of cable theory in which the potential in the extracellular medium (the lumen of the T-system) was taken to be radially symmetrical, the potential in the intracellular medium (the sarcoplasm) being radially uniform. Although most plausible, the great advantage of this approach was the simplicity of the result, not the rigor of its derivation: the approach allows the description of the T-system without seriously complicating the one-dimensional description of the cylindrical muscle fiber.

The work presented here can be viewed as a synthesis of the previous work on syncytia and on the T-system of skeletal muscle. On the one hand, the potentials are described by a pair of coupled Klein-Gordon equations; on the other hand, the perturbation analysis establishes (instead of assuming) a set of approximations equivalent to those customarily used in skeletal muscle.

Mathematical Approximations

Certain features of the analysis require further comments. The derivation presented is reasonably precise, sharing many of the difficulties that any derivation of a smoothed representation of a fundamentally discrete (i.e. quantized) system must have. We expect the derivation, and therefore probably the results, to break down when the discrete properties of the preparation are important. For example, if one were recording with two microelectrodes within one of the cells which make up the preparation (or with a single microelectrode with circuitry to compensate for the electrode impedance), one would expect the theory to be inadequate because the internal resistivity of a single cell would determine the flow of intracellular current near the electrode(s), not the effective resistivity of the entire preparation. Indeed, in this particular situation even the precise pattern of connections between cells might be significant. Similarly, we expect the theory to be of restricted use at frequencies (or under conditions or at times) for which the decrement of potential is steep compared to cell size. For example, when l/γ approaches a cell size in magnitude, one expects the equations describing the preparation to change qualitatively. In the case of the lens such would be the case around 500 Hz, and it may seem surprising that experimental results (Mathias et al., 1979) do not show more dramatic deviations from the theory at those frequencies. However, in a somewhat analogous situation (the tubular system of frog muscle), Mathias et al. (1977) have shown that the discrete properties of their system have a more quantitative than qualitative effect in an equivalent frequency range. Indeed, in the case of the T-system it proved possible to incorporate the effects of the discrete nature in a surprisingly simple way. We can hope that a similar generalization will be possible here, at least for the dominant terms $U_i^{(0)}$ and $U_c^{(0)}$, or the general term with the current electrode in the center of the preparation. In those situations there may well be enough congruence between the symmetry of the electric field and the preparation to allow analysis of the discrete effects.

It is difficult to state with precision the mathematical range of validity of the analysis, as it is difficult to state the precise range of validity of any expansion involving a number of independent parameters, which can combine in a large number of ways. Different combinations of parameters in our problem can, for example, represent (in an approximate sense) everything from an infinite resistive solid to a single spherical cell with a purely capacitive outer membrane, each having, of course, different behavior as a function of frequency. Physically, it is clear that the approximations used here (which are summarized in the circuits in Fig. 6) have a wide range of validity. Mathematically, it is clear that the requirements of small ϵ and small $\kappa\epsilon$ are met, at least for the lens. In the lens $\kappa\epsilon \rightarrow 1$ only at frequencies of the order of 1 MHz. There is also no doubt, however, that the solution has frequency dependence in addition to that just described; for example, the direct effects of the point source of current cannot be described simply by a series resistance at all frequencies. Further discussion of the range of validity of our approximation requires, however, an explicit analysis of the frequency dependence of the exact solution of the system of partial differential equations, which analysis is not yet available. We can be sure now that the solutions are "low" frequency approximations. But we cannot precisely define low frequency.

The restriction to "low" frequencies has certain consequences for the interpretation of

the step function response given in Fig. 5. The curves shown are computed from the first two terms in the perturbation expansion; they cannot rigorously be equated with the response of the original set of equations to a step current. In a somewhat analogous case, however, Peskoff and Eisenberg (1975) showed that the transient response so predicted was the appropriate approximation to the exact transient response, in the range of times of physiological interest.

Structural and Physiological Assumptions

The goal of this paper is to represent a syncytial tissue consisting of electrically coupled cells and a pervading extracellular space by an electrical model, an electrical model simple enough to understand in physical terms and realistic enough to use in physiological situations. The particular tissue we have had in mind is the lens of the eye, although spherical preparations of cultured cardiac muscle are probably just as well described by the model. The lens of the eye undoubtedly has certain structural features and perhaps certain biophysical properties which have been simplified away in our analysis. For example, (a) the resistance of the couplings between cells has been treated as part of the internal resistivity of the cells; (b) only the outermost membrane of the outermost cell layer has been allowed to have different properties from the internal membranes; that is, no systematic radial gradient of membrane properties has been permitted; (c) the anterior layer of cuboidal epithelium has not been included; (d) the anisotropy permitted is of a limited type which may not adequately describe the anisotropy expected from the structure of the lens.

The first simplification, the precise description of the resistive contribution of the gap junctions (particularly, to nonuniform or *anisotropic* properties), will require mapping of the locations of those junctions, a nontrivial task. It seems safe, however, to conclude that the junctions will contribute only resistive (not capacitive) properties at the frequencies of interest here. It is possible to estimate the natural frequency of the gap junction (the frequency at which the capacitive properties become important) from measurements and some elementary considerations. The effective resistivity R , due to both gap junctions and cytoplasm is some 625 ohm · cm (Table I and Eq. 7). As the actual cytoplasmic resistivity is at least $\frac{1}{3}$ of this figure, this effective resistivity is produced primarily by the series resistance of $1/(2.4 \times 10^{-4})$ gap junctions, because the size of a lens fiber (in the radial direction) is some 2.4 μm . Thus, the membrane resistance of the gap junctions, if they occupied the entire fiber membrane, would be about 0.15 ohm · cm², giving a natural frequency, in conjunction with a double thickness of membrane (capacitance about 0.5 $\mu\text{F}/\text{cm}^2$), of 2 MHz. Of course, this is a lower bound. Only a part of the fiber membrane is involved in gap junctions, because most of the membrane (and capacitance) separates the intra- and extracellular media. Although direct measurements of the area of gap junction membrane are not available, an estimate of the natural frequency of a single junction can be made from structural studies of other preparations. Fig. 11 of Makowski et al. (1977) shows about a 1-nm diameter "hole" associated with an 8.5-nm hexagon of lipid bilayer, the hole being about 12 nm long. If the actual resistivity of the cytoplasm is some 200 ohm · cm, one can estimate the impedance of one gap junction to be 10^{11} ohm in parallel with a capacitance of about 3×10^{-19} F, giving a natural frequency of 5 MHz.

Another troublesome aspect of this analysis concerns the meaning of the boundary condition. It seems likely to us that the parameters in the boundary condition represent the

composite properties of membranes in the outermost layer of lens fibers, a layer of size corresponding to the volume element shown in Fig. 1. In that case it would be incorrect to interpret the "surface" properties as those of a single membrane; the correct physiological interpretation would require a more precise mathematical analysis of the meaning of the boundary condition than is currently available.

There is no doubt that future work is needed to test and extend this model; in particular, to find which of the listed approximations and simplifications limit the applicability of the model to the real situation. The ability of the model to describe rather complex electrical properties is quite good (Mathias et al., 1979), however, and leads us to expect that in a general sense the model will remain useful. Indeed, one can even hope that models of this general type will be useful to describe the variety of syncytial tissues, of different geometry and function, which seem to use electrical current in their natural function.

A recent analysis of a cylindrical syncytium (Peskoff, 1978b) begins this process by

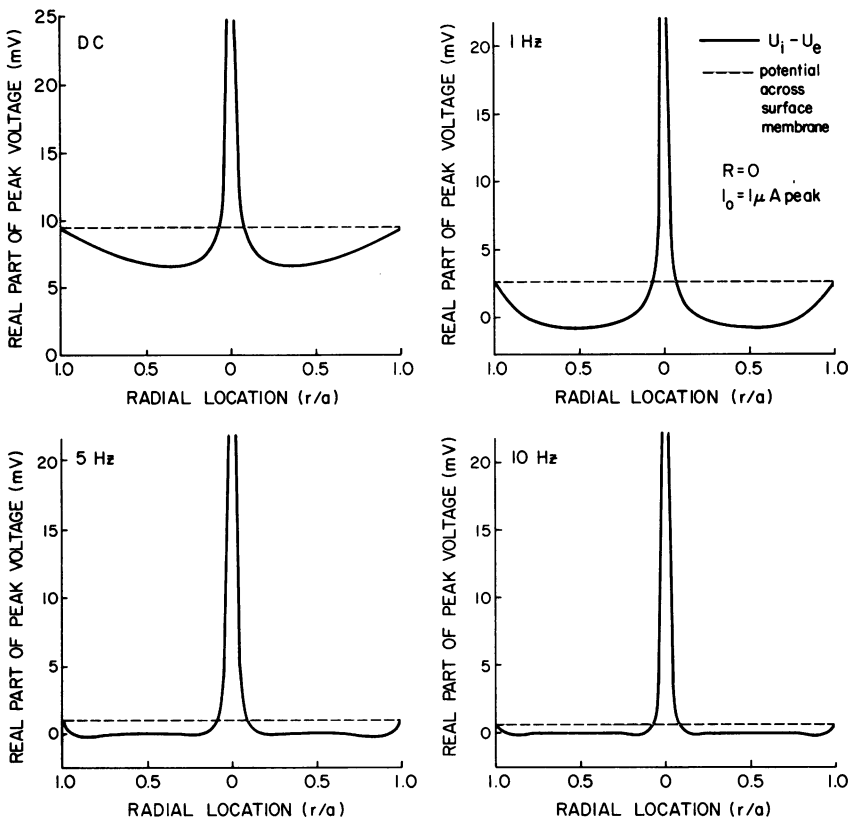


FIGURE 7 The spatial variation of transmembrane potential within the lens, a spherical syncytium. Each panel illustrates (solid line) the spatial variation of the potential $U_i - U_e$, the potential across the inner membranes of the syncytium. The potential across the surface membrane (dashed line), which closely approximates $U_i^{(0)}$ in the present case, is also shown to emphasize the deviations from uniformity: the potential across the inner membranes cannot be approximated by the potential across the surface membrane, even at DC. The parameters used in the calculation are given in Table I and on the figure itself. Eqs. 13-22 and 51 were used in the calculation. The dependence of frequency is subject to uncertainties described in the Discussion.

describing the transverse tubular system of a skeletal muscle fiber as an isotropic system of inner membranes and tubules. The structure of the transverse tubular system in skeletal muscle is highly anisotropic, however, and all other analyses, following Falk and Fatt (1964), have neglected longitudinal current in transverse tubules. Such longitudinal currents have also been neglected in the analysis of the clefts of cardiac Purkinje fibers (Schoenberg et al., 1975). Recently, Mathias (1978) has analyzed the current flow in a circuit model of the helicoidal tubular system of skeletal muscle. The analysis showed that longitudinal current in the tubular system was quite negligible. Thus, an analysis of the cylindrical syncytium must deal with a highly anisotropic extracellular medium, perhaps profitably using the approach of Appendix II.

Implications: Lens and Cardiac Muscle

The implications of this model for the function of the lens are discussed in a paper (Mathias et al., 1979) devoted to the confrontation of the model with experimental reality. One implication of the model for spherical preparations of cardiac muscle is shown in Fig. 7. This figure illustrates the spatial variation of membrane potential expected in a spherical preparation with the current electrode at its center. The solid line describes $U_i - U_e$, from Eqs. 13 and 21. The dashed line describes the potential across the outer membrane $U_i(r = a; R = 0)$, which is very close to $U_i^{(0)}$ for the parameters given in Table I. Note that even at DC there is poor spatial uniformity of potential; at higher frequencies there are essentially no regions of the inner membranes of the same potential as the surface membrane. This figure has been computed for the lens, with its very long time constant of a second. However, similar situations are likely in other spherical preparations at frequencies that bear the same relation to the time constant of that preparation. It certainly seems a remote possibility that other spherical preparations will be "space clamped" (i.e. have uniform potentials across all membranes) at times comparable to their time constant. Thus, voltage clamp experiments of spherical syncytia must be interpreted without assuming such space clamped conditions.

APPENDIX I

Proof of Reciprocity

The proof of reciprocity for our system of equations uses the techniques developed to prove reciprocity for Laplace's equation or the Helmholtz equation (Morse and Feshbach, 1953, p. 808). We first write Eq. 27 twice, once with a source at \vec{R}_0 and once with a source at \vec{R}_1 . The equation for the source at \vec{R}_0 is multiplied by $U_i(\vec{r} | \vec{R}_1)$ and the equation with the source at \vec{R}_1 is multiplied by $U_i(\vec{r} | \vec{R}_0)$.⁴ The multiplied equations are subtracted and integrated to give

$$\begin{aligned} & \iiint_{\text{tissue}} \{U_i(\vec{r} | \vec{R}_1) \cdot \nabla^2 U_i(\vec{r} | \vec{R}_0) - U_i(\vec{r} | \vec{R}_0) \cdot \nabla^2 U_i(\vec{r} | \vec{R}_1)\} dV \\ & + \epsilon \iiint_{\text{tissue}} \{U_i(\vec{r} | \vec{R}_1) U_e(\vec{r} | \vec{R}_0) - U_i(\vec{r} | \vec{R}_0) U_e(\vec{r} | \vec{R}_1)\} dV \\ & = U_i(\vec{R}_1 | \vec{R}_0) - U_i(\vec{R}_0 | \vec{R}_1). \quad (55) \end{aligned}$$

⁴The solidus (|) is used to separate the location of the source (to the right) from the point at which potential is measured (to the left).

Application of Green's theorem (Morse and Feshbach, 1953, p. 803) and substitution from Eq. 28 give another expression for the difference of potentials:

$$\begin{aligned}
 & U_i(\vec{\mathbf{R}}_1 | \vec{\mathbf{R}}_0) - U_i(\vec{\mathbf{R}}_0 | \vec{\mathbf{R}}_1) \\
 &= \iint_{\text{surface}} \left\{ U_i(\vec{\mathbf{r}} | \vec{\mathbf{R}}_1) \frac{\partial U_i(\vec{\mathbf{r}} | \vec{\mathbf{R}}_0)}{\partial \mathbf{r}} - U_i(\vec{\mathbf{r}} | \vec{\mathbf{R}}_0) \frac{\partial U_i(\vec{\mathbf{r}} | \vec{\mathbf{R}}_1)}{\partial \mathbf{r}} \right\} d\vec{\mathbf{S}} \\
 &- \frac{\epsilon}{1 - \epsilon} \iint_{\text{surface}} \left\{ U_e(\vec{\mathbf{r}} | \vec{\mathbf{R}}_0) \frac{\partial U_e(\vec{\mathbf{r}} | \vec{\mathbf{R}}_1)}{\partial \mathbf{r}} - U_e(\vec{\mathbf{r}} | \vec{\mathbf{R}}_1) \frac{\partial U_e(\vec{\mathbf{r}} | \vec{\mathbf{R}}_0)}{\partial \mathbf{r}} \right\} d\vec{\mathbf{S}}. \quad (56)
 \end{aligned}$$

The boundary conditions (Eqs. 29 and 30) ensure that each integral is equal to zero for all values of ϵ , independent of the spatial location of the sources. Then, we have the result

$$U_i(\vec{\mathbf{R}}_1 | \vec{\mathbf{R}}_0) = U_i(\vec{\mathbf{R}}_0 | \vec{\mathbf{R}}_1). \quad (57)$$

Because \mathbf{R}_1 and \mathbf{R}_0 can describe any location, the theorem is proved. The use of Green's theorem has "integrated out" the dependence on the original observation point \mathbf{r} and replaced it with one of the original source locations. The procedure of successive limits, defined near Eq. 32, shows that reciprocity is satisfied individually by each component $U_i^{(n)}$ of the total intracellular potential.

APPENDIX II

The Anisotropic Case

Our analysis can be extended without too much difficulty to the anisotropic case in which the *effective* resistivities R_i and R_e are allowed to have one pair of values in the radial direction and another pair of values in the angular directions perpendicular to the radial direction. This situation is likely to occur in spherically symmetrical biological preparations, for example, a smoothed representation of the lens of the eye, or in the overly examined *Allium cepa*.

We represent the angular component of the Laplacian by L^2 . β_i is the ratio of the effective intracellular resistivity in the radial direction (now called R_i) to the effective intracellular resistivity in the angular direction. β_e is the ratio of the effective extracellular resistivity in the radial direction (now called R_e) to the effective extracellular resistivity in the angular direction. The dimensionless version of the differential equations and boundary conditions is then

$$\left(\frac{\partial^2}{\partial \mathbf{r}^2} + \frac{2}{\mathbf{r}} \frac{\partial}{\partial \mathbf{r}} + \frac{\beta_i}{\mathbf{r}^2} L^2 \right) U_i - \epsilon(U_i - U_e) = -\epsilon \delta(\vec{\mathbf{r}} - \vec{\mathbf{R}}) \quad (58)$$

$$\left(\frac{\partial}{\partial \mathbf{r}^2} + \frac{2}{\mathbf{r}} \frac{\partial}{\partial \mathbf{r}} + \frac{\beta_e}{\mathbf{r}^2} L^2 \right) U_e + (1 - \epsilon)(U_i - U_e) = 0 \quad (59)$$

$$\left. \begin{aligned} \frac{\partial U_i}{\partial \mathbf{r}} + \kappa \epsilon U_i &= 0 \\ U_e &= 0 \end{aligned} \right\} \text{on } \mathbf{r} = \gamma a \quad (60)$$

$$U_e = 0 \quad (61)$$

where the structure has been assumed to be axially symmetric, independent of longitude and where

$$L^2 = \frac{1}{\sin \theta} \frac{\partial}{\partial \theta} \left(\sin \theta \frac{\partial}{\partial \theta} \right). \quad (62)$$

Substitution of the expansions (Eqs. 29 and 30) into the differential equations shows that the prob-

lems defining $U_i^{(0)}$ and $U_e^{(0)}$ are unchanged by the inclusion of anisotropy, the meaning of the variables R_i and R_e simply being restricted in the anisotropic case to the effective radial resistance. The problem defining $U_i^{(1)}$ is changed but in a surprisingly simple manner. If $\bar{U}_i(\mathbf{r})$ is defined as the angular average of $U_i^{(1)}(\mathbf{r}, \theta)$ the numerical superscripts being suppressed for simplicity, we have

$$\bar{U}_i = \frac{1}{2} \int_0^\pi U^{(1)}(\mathbf{r}, \theta) \cdot \sin \theta \, d\theta \quad (63)$$

$$U_i^{(1)} = \bar{U}_i(\mathbf{r}) + \tilde{U}_i(\mathbf{r}, \theta). \quad (64)$$

Problems can then be written for the symmetric (i.e. the radial) and angular parts of $U_i^{(1)}$

$$\begin{cases} \frac{\partial^2 \bar{U}_i}{\partial r^2} + \frac{2}{r} \frac{\partial \bar{U}_i}{\partial r} = \frac{-1}{4\pi r^2} \delta(\mathbf{r} - \mathbf{R}) + U_i^{(0)} - U_e^{(0)} \\ \frac{\partial \bar{U}_i}{\partial r} = -\kappa U_i^{(0)} \quad \text{on } r = \gamma a \end{cases} \quad (65)$$

$$\begin{cases} \frac{\partial^2 \tilde{U}_i}{\partial r^2} + \frac{2}{r} \frac{\partial \tilde{U}_i}{\partial r} + \frac{\beta_i}{r^2} L^2 \tilde{U}_i = \frac{-\delta(\mathbf{r} - \mathbf{R})}{2\pi r^2} \left[\frac{\delta(\theta)}{\sin \theta} - \frac{1}{2} \right] \\ \frac{\partial \tilde{U}_i}{\partial r} = 0 \quad \text{on } r = \gamma a \end{cases} \quad (66)$$

The radial problem can be solved directly or compared with problems previously solved (Eq. 47) to give the result, in dimensional form,

$$U_i = \psi(r) + \psi(R) + C_1 + \frac{I_0(R_i + R_e)}{4\pi} \left[\frac{R + r - |R - r|}{2Rr} - \frac{1}{a} \right]. \quad (67)$$

The last term of the right-hand side of Eq. 67 is the angular average of R_s (see footnote 2). $\psi(\cdot)$ is defined in Eq. 19. The constant C_1 can be shown to equal $-2C_0$ by separating the anisotropic intracellular and extracellular potentials into angular and radial parts and applying the integration procedure previously described (see Eq. 43).

The angular component of the dimensional potential $U_i^{(1)}$ can be determined by standard methods:

$$\begin{aligned} \tilde{U}_i^{(1)} = \frac{I_0(R_i + R_e)}{4\pi a} \sum_{m=1}^{\infty} \frac{2n+1}{2\nu+1} \frac{(rR)^\nu}{a^{2\nu}} \\ \left[\frac{1+\nu}{\nu} + \left(\frac{2a}{R+r+|R-r|} \right)^{2\nu+1} \right] P_m(\cos \theta) \end{aligned} \quad (68)$$

where

$$\nu = -\frac{1}{2} + \left(\frac{1}{2}\right) \sqrt{4n(n+1)\beta_i + 1}. \quad (69)$$

The isotropic case occurs when $\beta_i = 1$ and so $\nu = n$. In that case \tilde{U}_i , written as $\tilde{U}_i(\nu = n)$, can be written in closed form, using Eq. 20 to express the closed form of R_s :

$$I_0 R_s - \frac{I_0(R_i + R_e)}{4\pi} \left[\frac{R + r - |R - r|}{2Rr} - \frac{1}{a} \right] = \tilde{U}_i(\nu = n). \quad (70)$$

Computation of the angular component \tilde{U}_i using the expansion, Eq. 68, should be easier (i.e. require fewer terms) if the singular behavior of the corresponding isotropic component is removed from the sum. That is to say, the left-hand side of Eq. 70 should be subtracted from the left-hand side of Eq. 68, and the right-hand side of Eq. 70 should be subtracted from the right-hand side of Eq. 68. In the subtraction of the two equations, the closed form (Eq. 20) of R_s , but the expanded form of \tilde{U}_i (from Eq. 68 with $\nu = n$), is used. To avoid numerical ill conditioning on the right-hand side, one should perform the subtraction within the brackets of the summand, before multiplication by the Legendre polynomial and before summation.

There are several noteworthy properties of the solution for the anisotropic case. First, the frequency-independent terms are the only terms influenced by the angular resistivity. Thus, the effects of the angular resistivity are confined to the easily measured series resistance term. Second, the series resistance term is modified in the presence of anisotropy in a straightforward manner. The radial component of the series resistance depends only on the radial resistivity, whereas the angular component depends on both resistivities. Thus, experiments like those of Mathias et al., 1979, in which there is no angular component of potential because the current electrode is in the center of the preparation, will measure the radial component of the effective intracellular resistivity. On the other hand, experiments made with electrodes just under the outer surface of the preparation (e.g. Eisenberg and Rae, 1976) will measure a composite resistivity.

The anisotropy, which might be observed in syncytial preparations, seems more likely to arise from the structure of the preparations than from the specific properties of the intra- or extracellular solutions. Thus, the surface to surface ratios, the tortuosity factors, or the distribution of junctions between cells (all of which help determine the effective resistivities in Eq. 7), seem to us the most likely causes of anisotropy in syncytial preparations.

It is a pleasure to acknowledge the contributions of Dr. A. Peskoff in the original formulation of the differential equations, of Dr. J. Rae in the confrontation of the theory with experimental reality, of Mr. T. Streicher in the computation of the results, and of Mr. R. Levis in general discussion.

This work was supported by National Institutes of Health grant HL-20230 and National Science Foundation grant PCM76-18043.

Received for publication 24 February 1978 and in revised form 25 September 1978.

REFERENCES

- BARCILON, V., J. D. COLE, and R. S. EISENBERG. 1971. A singular perturbation analysis of induced electrical fields in nerve cells. *SIAM J. Appl. Math.* **21**:339.
- BARR, L., and E. JAKOBSSON. 1976. The spread of current in electrical syncytia. *In Physiology of Smooth Muscle*. E. Bulbring and M. F. Shuba, editors. Raven Press, New York.
- BENNETT, M. R. 1972. *Autonomic Neuromuscular Transmission*. Cambridge University Press, London.
- BRIGHAM, E. O. 1974. *The Fast Fourier Transform*. Prentice-Hall, Inc., Englewood Cliffs, N.J.
- CHANDLER, W. K., and M. F. SCHNEIDER. 1976. Time-course of potential spread along a skeletal muscle fiber under voltage clamp. *J. Gen. Physiol.* **67**:165.
- DE HAAN, R. L., and H. A. FOZZARD. 1975. Membrane response to current pulses in spheroidal aggregates of embryonic heart cells. *J. Physiol. (Lond.)* **65**:207.
- EISENBERG, R. S., V. BARCILON, and R. T. MATHIAS. 1978. Electrical properties of a spherical syncytium. *Biophys. J.* **21**:48a. (Abstr.)
- EISENBERG, R. S., R. T. MATHIAS, and J. L. RAE. 1977. Measurement, modeling, and analysis of the linear electrical properties of cells. *Ann. N. Y. Acad. Sci.* **303**:342.
- EISENBERG, R. S., and J. L. RAE. 1976. Current-voltage relationships in the crystalline lens. *J. Physiol. (Lond.)* **262**:285.
- FALK, G., and P. FATT. 1964. Linear electrical properties of striated muscle fibers observed with intracellular electrodes. *Proc. R. Soc. Lond. Biol. Sci.* **160**:69.
- FROMTER, E. 1972. The route of passive ion movement through the epithelium of Necturus gallbladder. *J. Membr. Biol.* **8**:259.

- HAYLETT, D. G., and D. H. JENKINSON. 1972. Effects of noradrenaline on potassium efflux, membrane potential and electrolyte levels in tissue slices prepared from guinea-pig liver. *J. Physiol. (Lond.)* **225**:721.
- JACK, J. J. B., D. NOBLE, and R. W. TSIEN. 1975. *Electric Current Flow in Excitable Cells*. Clarendon Press, Oxford.
- KELLOGG, O. D. 1929. *Foundations of Potential Theory*. Dover Publications Inc., New York.
- MAKOWSKI, L., D. L. D. CASPAR, W. C. PHILLIPS, and D. A. GOODENOUGH. 1977. Gap junction structures. II. Analysis of the x-ray diffraction data. *J. Cell Biol.* **74**:629.
- MATHIAS, R. T. 1978. An analysis of the electrical properties of a skeletal muscle fiber containing a helicoidal T-system. *Biophys. J.* **23**:277.
- MATHIAS, R. T., R. S. EISENBERG, and R. VALDIOSERA. 1977. Electrical properties of frog skeletal muscle fibers interpreted with a mesh model of the tubular system. *Biophys. J.* **17**:57.
- MATHIAS, R. T., J. RAE, and R. S. EISENBERG. 1979. Electrical properties of structural components of the crystalline lens. *Biophys. J.* **25**:181-201.
- MATTHEWS, E. K., and Y. SAKAMOTO. 1975. Electrical characteristics of pancreatic islet cells. *J. Physiol. (Lond.)* **246**:421.
- MORSE, P., and H. FESHBACH. 1953. *Methods of Theoretical Physics*. McGraw-Hill Book Company, New York.
- PESKOFF, A. 1978a. Electric potential in three-dimensional electrically syncytial tissues. *Bull. Math. Biophys.* In press.
- PESKOFF, A. 1978b. Electric potential in cylindrical syncytia and muscle fibers. *Bull. Math. Biophys.* In press.
- PESKOFF, A., and R. S. EISENBERG. 1973. Interpretation of some microelectrode measurements of electrical properties of cells. *Ann. Rev. Biophys. Bioeng.* **2**:65.
- PESKOFF, A., and R. S. EISENBERG. 1975. The time-dependent potential in a spherical cell using matched asymptotic expansions. *J. Math. Biol.* **2**:277.
- PESKOFF, A., R. S. EISENBERG, and J. D. COLE. 1976. Matched asymptotic expansions of the Green's function for the electrical potential in an infinite cylindrical cell. *SIAM J. Appl. Math.* **30**:222.
- PETERSEN, O. H. 1974. Electrophysiological studies on gland cells. *Experientia (Basel)*. **30**:130.
- PURVES, R. D. 1976. Current flow and potential in a three-dimensional syncytium. *J. Theor. Biol.* **60**:147.
- RAE, J. L. 1978. The electrophysiology of the crystalline lens. In *Current Topics in Eye Research*. Vol. 1. Academic Press, Inc., New York.
- SCHEY, H. M. 1973. *Div, Grad, Curl, and All That*. W. W. Norton & Company, Inc., New York.
- SCHOENBERG, M., G. DOMINGUEZ, and H. A. FOZZARD. 1975. Effect of diameter on membrane capacity and conductance of sheep cardiac Purkinje fibers. *J. Gen. Physiol.* **65**:441.
- SHAW, T. I. 1964. Core conductor properties of tissue reticulum. In *A Collection of Papers Presented to Sir Charles Lovatt Evans*. C.D.E.E. Press.
- SHERIDAN, J. D. 1971. Electrical coupling between fat cells in newt fat body and mouse brown fat. *J. Cell Biol.* **50**:795.
- SOBOLEV, S. L. 1964. *Partial Differential Equations of Mathematical Physics*. Addison-Wesley Publishing Company Inc., Reading, Mass.
- WEIDMANN, S. 1966. The diffusion of radiopotassium across intercalated disks of mammalian cardiac muscle. *J. Physiol. (Lond.)* **187**:323.